

The Improved Velocity-based Models for Pedestrian Dynamics

Xiao Yang¹, Zheng Qin¹, Binhua Wan², Renwei Zhang¹ and Huihui Wang³

¹ School of Software and TNList, Tsinghua University, Beijing, China
[e-mail: yangxiao356@126.com, iveryoung@163.com, anyrenwei@163.com]

² First Hospital of Tsinghua University, Tsinghua University, Beijing, China
[e-mail: wanbiangde@qq.com]

³ Department of Engineering, Jacksonville University, Jacksonville, Florida Area 261, US
[e-mail: hwang1@ju.edu]

*Corresponding author: Xiao Yang, Zheng Qin, Binhua Wan

*Received March 5, 2017; revised April 20, 2017; accepted May 5, 2017;
published September 30, 2017*

Abstract

Three different improvements of the Velocity-based model were proposed in a minimal velocity-based pedestrian model. The improvements of the models are based on the different agent forms. The different representations of the agent lead to different results, in this paper, we simulated the pedestrian movements in some typical scenes by using different agent forms, and the agent forms included the circles with different radiuses, the ellipse and the multi-circle stand for one pedestrian. We have proposed a novel model of pedestrian dynamics to optimize the simulation. Our model specifies the pedestrian behavior using a dynamic ellipse, which is parameterized by their velocity and can improve the simulation accuracy. We found a representation of the pedestrian much closer to the reality. The phenomena of the self-organization can be observable in the improved models.

Keywords: Dynamic ellipse, Velocity-based, Slow Reaction, Pedestrian distribution

1. Introduction

For more efficient and safe evacuation of pedestrians in the interior, the stable and empirical-based models are required. Up to now, the research on pedestrian dynamics can be divided into macroscopic models (e.g. the models based on hydrodynamics) and microscopic models (e.g. the Lattice Gas model), the microscopic models usually set the pedestrians as autonomous agents, it can be divided into discrete models (e.g. the Floor-field model based on cellular automata) and continuous models (e.g. the Force-based model based on the Newton's law). The models based on Cellular Automata always operated with discrete in space, while the force-based models present spatially continuous features.

$$m_i \ddot{R}_i = \vec{F}_i = \overline{F}_i^{drv} + \sum_{j \in N_i} \overline{F}_{ij}^{rep} + \sum_{w \in W_i} \overline{F}_{iw}^{rep} \quad (1)$$

Force-based models have been strongly developed in the last five years, it takes Newton's second law as a guiding principle and describes the interactions of pedestrians in terms of physical and social forces, the trajectories of pedestrians are defined by the differential equations [1], [2], [3].

The force-based models are second-order models. Equation (1) shows a representative ODE (ordinary differential equation) of the force-based model, we can get the messages such as velocity and direction by setting the proper initial value and parameters.

As we all know, there are many solutions corresponding to the second-order ODEs, including the Euler method, the improved Euler method and the Runge-Kutta method et al.

The Euler method is a numerical procedure for solving ODEs and commonly used in with a given initial value. It is the most basic and simple method for integration of ODEs. The approximation computed by Euler method has deviations compared to the actual value.

The Velocity-based models are great progress of the Force-based models, they're first-order models, the ODEs usually presents like the (2). The collision-free speed model [4] proposed by A. Tordeux solves the dilemma of overlapping and oscillations in force-based models and reduces the computation cost.

Table 1. Symbol Description (Velocity Based Model)

Symbol	Description
x_i	Pedestrian position
v_i	Pedestrian speed

θ_i	Pedestrian direction
$s_{i,j}$	$\ x_i - x_j\ $
l	Pedestrian size= $2 \times$ Radium
$e_{i,j}$	Unit vector from x_j to x_i
e_i	$(\cos \theta_i, \sin \theta_i)$
v_0	1.2m/s
l	0.3m
T	1s
a	5
D	0.1m

$$\dot{x}_i = V(x_i, x_j, x_k, \dots) \tag{2}$$

Some illuminating ideas of the existing first order pedestrian models such as the Gradient navigation model with additive neighbor repulsions [5], Synthetic vision-based model based on time-to-interaction and bearing angle [6] and Velocity obstacle approach borrowed from robotic [7] are added to optimize the velocity-based models.

The reproductions of the collective phenomena are important qualitative evaluation criteria to estimate the pedestrian model, the collective phenomena usually include the stop and go wave, phase-transition, lane formation, Oscillations at bottleneck, clogging at exit doors and so on [2], [8]. The Lane formation and Oscillations at bottleneck phenomena are showed in Fig. 1 and Fig. 2.

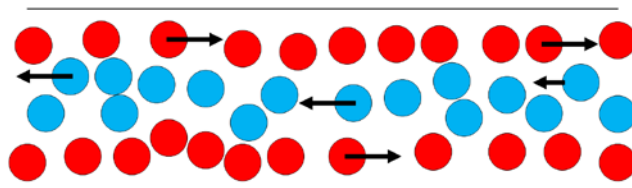


Fig. 1. Lane formation

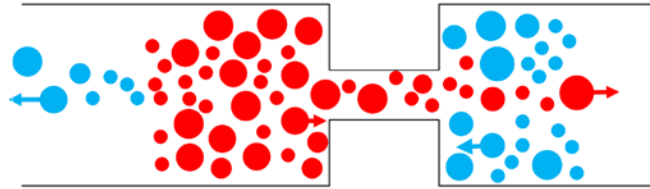


Fig. 2. Oscillations at bottleneck

The general quantitative evaluation criteria of the pedestrian models are the fundamental diagrams [9], [10], [11], [12], constituted by the density and velocity of the model. The different rough sketches in Fig. 3 corresponding to the different pedestrian models or scenes.

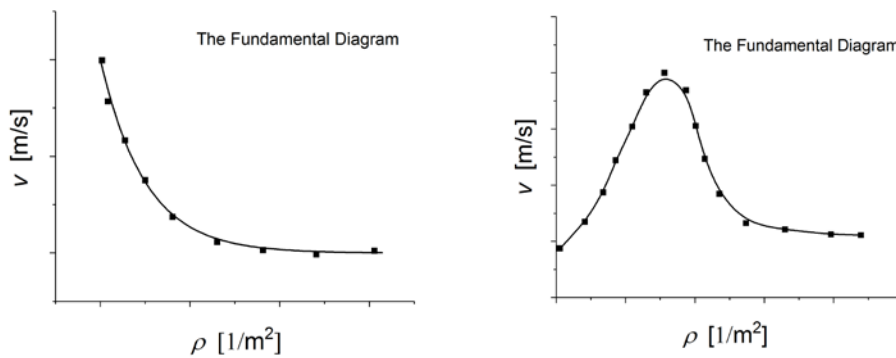


Fig. 3. The common fundamental diagram

In this work, we lay emphasis on the improvements of the velocity-based model without overlapping or oscillation. The classic self-organization phenomena based on empirical research or simulations of force-based models are reproduced by our model.

2. The Improved Velocity-based Pedestrian Model

According to the Antoine's research [4], the circle shape velocity-based model is shown in Fig. 4. The equation of a continuous velocity model can be presented as,

$$\dot{x}_i = V(x_i, x_j, x_k, \dots) \times e_i(x_i, x_j, x_k, \dots) \quad (3)$$

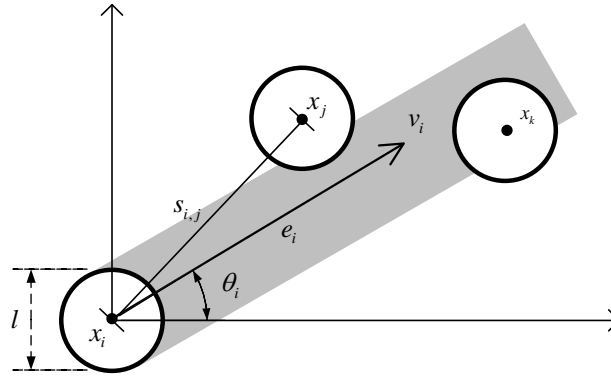


Fig. 4. Sketch map

2.1 Definition of the velocity-based model

Antoine [4] proposed the optimal velocity (OV) model based on spacing in front of the pedestrian, and the concept “repulsion” is mainly depend on the spacing in front. The OV model is borrowed from road traffic model [13], [14], which is constructed in a simple concept: A driver maintains the optimal velocity depending on the distance to other vehicles. Similarly, a pedestrian keeps the optimal velocity depending on the spacing to other pedestrians.

In Antoine’s model [4], the set of the pedestrians in front of pedestrian i is defined by

$$J_i = \{j, e_i \cdot e_{i,j} \leq 0 \text{ and } |e_i^\perp \cdot e_{i,j}| \leq l/s_{i,j}\}. \tag{4}$$

The minimum distance in front s_i

$$s_i = \min_{j \in J_i} s_{i,j} \tag{5}$$

Moreover, the model can be expressed as

$$\dot{x}_i = V(s_i(x_i, x_j, x_k, \dots)) \times e_i(x_i, x_j, x_k, \dots) \tag{6}$$

While the V stands for the OV function and e_i represents the direction model.

The model is collision-free with v_0 the desired velocity and T the time gap, so the V can be computed as:

$$V(s) = \begin{cases} 0, & s \leq l \\ \frac{s-l}{T}, & 0 \leq \frac{s-l}{T} \leq v_0 \\ v_0, & v_0 \leq \frac{s-l}{T} \end{cases} \tag{7}$$

The direction e_i based on a repulsion function depending on the distances ($s_{i,j}$) between the adjacent pedestrians.

$$e_i(x_i, x_j, x_k, \dots) = \frac{1}{N} (e_0 + \sum_j R(s_{i,j}) e_{i,j}) \tag{8}$$

$$R(s_{i,j}) = a \exp\left(\frac{l-s_{i,j}}{D}\right) \tag{9}$$

With e_0 the desired direction, a the repulsion rate and D the repulsion distance. Overall, five parameters need to set in Antoine’s model , in his research the parameters is setting to the optimal value.

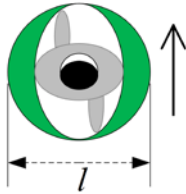
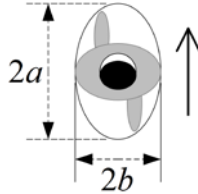
2.2 Hard Circles, Hard Ellipse and Dynamical Ellipse

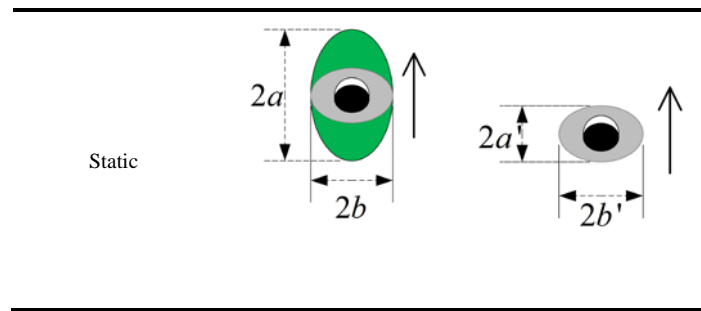
According to the paper [15], [16], [17], [18], there is still a controversy in pedestrian shapes when simulating the pedestrian dynamics. The hard circles are most used in the continuous models such as force-based model, [16] found that pedestrians with different speed usually occupy different space, the faster the pedestrian, the more space he will occupy, a linear velocity-dependence of radius was proposed as $r = r_{min} + \tau v$ and proved better than the Hard Circle models. However, the drawback of the circles is that they are rotational symmetry, which means they occupy the same space in every direction, especially in two-dimensional movement the circles occupy unnecessary space as **Table 2** shown.

The green area is the redundant when we actually simulate the pedestrian dynamics, but the circles is still in common use when we perform a first order velocity-based model. What we can see from the **Table 2** is that the space, which the moving pedestrian occupied, is similar to the ellipse paralleling to the moving direction and the space that the stationary or low-speed pedestrians take up is more similar to the ellipse orthogonal to the moving direction. Therefore, the ellipses is better than the circles to modelling and simulating the pedestrian dynamics, it is closer to the reality.

Antoine’s velocity-based model [4] using hard circles for its simplicity and straightforward, we have improved the pedestrian shape from the Common one to the Better one by using the ellipse shape, and the **Fig. 4** can be changed to **Fig. 5**.

Table 2. Pedestrian Project Shape

State	Common	Better
Dynamic		



We can see from the sketch map in **Fig. 6**, pedestrian x_k was in the passing area (grey area in **Fig. 6**) of pedestrian x_i when we using the circles, as the circles turned into ellipses, the lateral area of the pedestrian is eliminated and x_k was out of the passing area when we using the ellipses. The pedestrian is “smaller” in ellipse models to some extent, consequently, the advantage is that there may be fewer interactions between pedestrians.

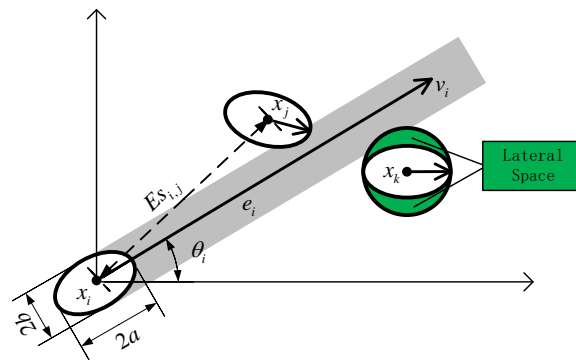


Fig. 5. Dynamic sketch map

2.3 The Slow Reaction Model

The concept of reaction time or response time is borrowed from the slow-to-start traffic model[19], and has been widely studied in last several years, Fang[9] applied the idea to Lattice-Gas model and proposed Slow-Reaction model. We can get this phenomenon from both Seyfried’s research [11] and the video of experiment, when the pedestrian flow at high density, the velocity of individual is very small and pedestrian’s attention easily reduced. In this case, pedestrians often cannot keep pace with the movement of pedestrians ahead immediately, as shown in **Fig. 6**, circles in green represent the slow reaction pedestrians. In addition, the reaction sensitivity varies. These factors contribute to pedestrian’s imbalance distribution, the space between some pedestrians much larger than the mean spacing. Therefore, the reaction time is an essential factor of the pedestrian dynamic research nowadays.

Because of the same pedestrian velocity in Slow Reaction Model, Fang set a probability parameter to distinguish if the pedestrian is in a Slow Reaction state. We apply the idea above to the Velocity-based model and analyze the experiment results.

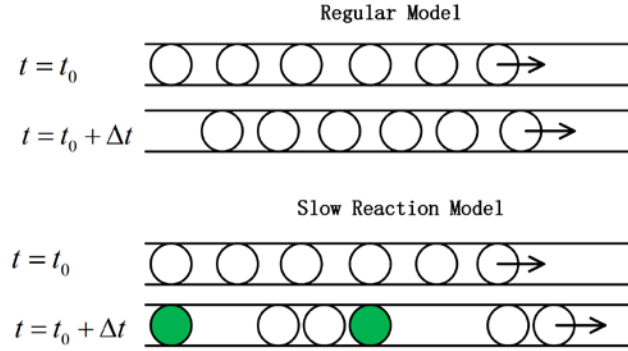


Fig. 6. Regular and Slow Reaction model

First, Similar to Fang’s Slow Reaction Model, we bring in a Slow Reaction probability p_i , the origin model can be described as:

$$x_i(t + \Delta t) = x_i(t) + \Delta t \times V(s_i(t))e_i(t) \times \varphi, \quad \varphi = \begin{cases} 0, & 1 - p_i \\ 1, & p_i \end{cases} \quad (10)$$

The pedestrian would go forward with a probability of p_i , and remain stationary with the probability $1 - p_i$.

2.4 The Initial Distribution of The Pedestrians In A Single Room

As we all know, the initial pedestrian distribution is an important factor to the evacuation efficiency, the most common used distribution of initial positions is the Uniform distribution, the experiments and simulations of Julich pedestrian laboratory [8] is mainly using this distribution. The Uniform distribution is always realized by dividing the room into squares, and making each square has roughly same number of pedestrians.

Moussa [20] have brought in three types of distribution in traffic model, it has an important influence in the network and security of intelligent transportation systems [21], [22]. Here we apply the different distributions into the velocity-based model, we choose the exit as each pedestrian’s destination, and distribute the distance between pedestrian and exit by an exponential distribution. The three exponential distribution in our experiment are respectively.

The exponential distribution:

$$f^e(\delta) = \frac{\mu}{e^{-\mu\delta m} - e^{-\mu\delta M}} e^{-\mu\delta} \quad (11)$$

The power-law distribution:

$$f^p(\delta) = \frac{k+1}{(\delta_M - \delta_m)^{k+1}} (\delta - \delta_m)^k \tag{12}$$

The uniform distribution:

$$f^u(\delta) = \frac{1}{\delta_M - \delta_m} \tag{13}$$

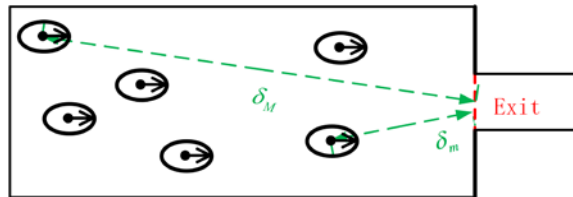


Fig. 7. Maximal distance δ_M and Minimal distance δ_m

Moussa define the parameter δ of the distance between the pedestrian and the exit, while δ_M and δ_m are respectively the minimal and maximal distance ,shown in **Fig. 7**, μ represents the characteristic length scale of the distribution.

We applied the three distributions in the bottleneck scene. Compared to experiments of **Fig. 8** ([5] ,[23], [10],), the parameters in our experiments depend on the empirical data from Seyfried and Schadschneider’s experiment [24], [8]. As shown in **Fig. 9**, the comparison experiment set $a = 2.8m, b = 1.2m, d = 3m$, the other parameters are same as Seyfried’s experiment [24].

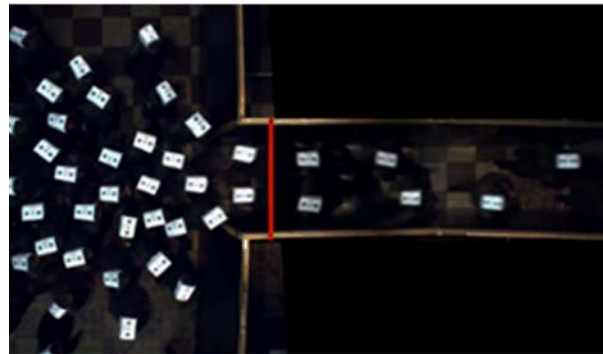


Fig. 8. Photo taken from Seyfried’s experiment

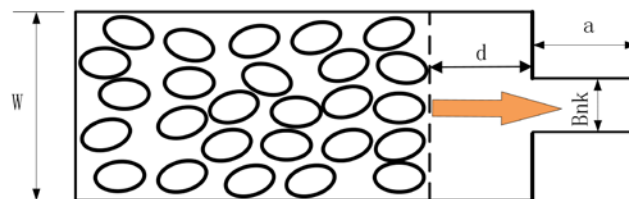


Fig. 9. Unidirection pedestrian flow with bottleneck

3. Experiment Result

We conduct our experiments in two scenes basically, one is the bottleneck scenario for comparing to the Seyfried's empirical data [24], the other is the bi-directional flows with bottleneck in rectangular scenario in contrast with Antoine's velocity model [4]. In order to make the results of comparison more meaningful, we set the parameters same as Seyfried's experiment and Antoine's experiment as much as possible.

In the Scenario A, we describe the experiment system with uni-directional flow with length $L = 7.5\text{m}$, width $W = 4\text{m}$, from random initial configurations and by using Euler numerical method with time step $dt=0.01\text{s}$. The other parameter settings are given in Table 1.

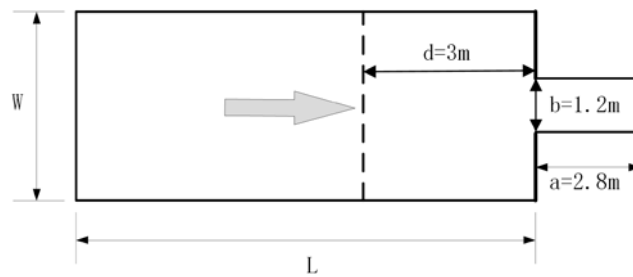


Fig. 10. Scenario A

In the Scenario B, the experiment system is with a bi-directional flow through a bottleneck, the parameters are similar to Antoine's experiment including length $L = 9\text{m}$, and width $W = 3\text{m}$ as shown in Fig. 10.

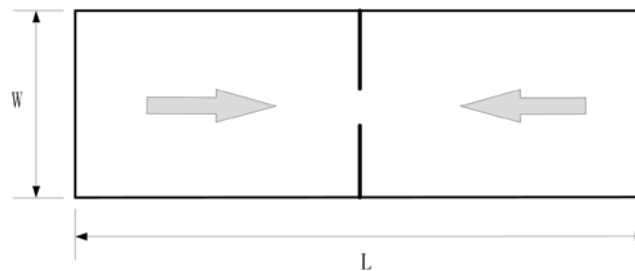


Fig. 11. Scenario B

3.1 Three Different Shapes Of The Pedestrian

The three models of pedestrian are in Fig. 13, we set the parameters in each experiment as followed: the hard circle model with $l = 0.3\text{m}$, same as Antoine's [4] velocity model; the hard ellipse model with $2a = 0.3\text{m}$, $2b = 0.2\text{m}$ and the dynamic ellipse model with $2a' = 2 \times (a'_{min} + \tau_a v)$, $a'_{min} = 0.18\text{m}$, $2b' = 0.2\text{m}$

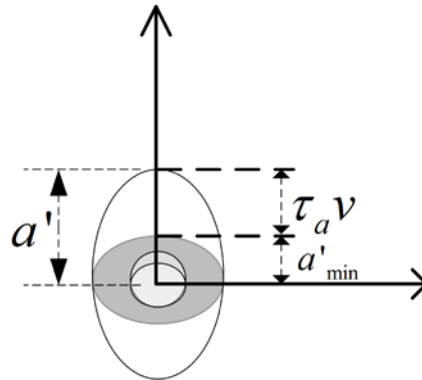


Fig. 12. Long axis and short axis of dynamic ellipse

Parameter τ_a is an adjustment coefficient to make sure that $2a' \leq 0.3m$, v can be computed as $V(s)$ from (8) in Section 2.1 and the value of a'_{min} is refer to ellipse model in force-based model [25].

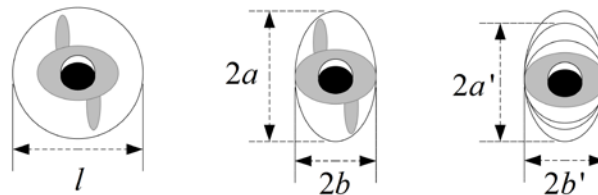


Fig. 13. The three types of pedestrian

We set the pedestrian number $N = 60$. The flow J is defined as number of pedestrians passing a settled location of the section per unit time and we compared the fundamental diagrams of three different shapes of the pedestrian in scenario A.

The three model pedestrian flow in different times are shown in Fig. 14. The Dynamic Ellipse model reveals the biggest flow, and in the bottleneck, the Ellipse and Dynamic Ellipse model both can hold three pedestrian in parallel in the bottleneck while the Circle model only hold for two. The velocity model is collision-free, so the pedestrians can just contact to each other, there are no overlaps in our experiments.

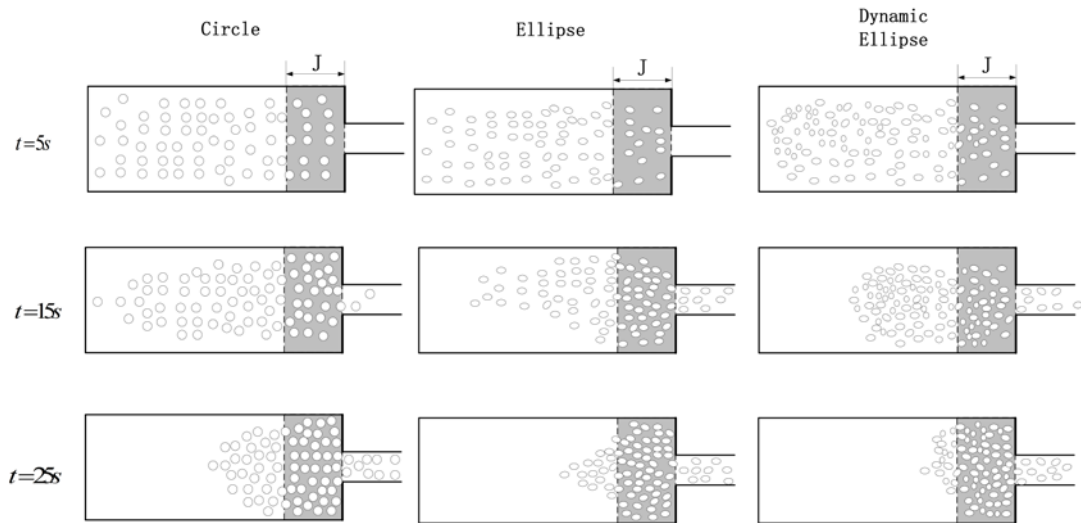


Fig. 14. Pedestrian evacuation in Scenario A using three types of shape



Fig. 15. Oscillation at bottlenecks in Scenario B

Fig. 16 compared the density-flow fundamental diagrams between the origin experiment by Seyfried and three transformed pedestrian models. We can see that the dynamic ellipse velocity-based model is much closer to the prototype, one reason for the deviations of the circle and ellipse model is the redundant area they occupied. The Circle and hard Ellipse model are widely used in continuous models such as force-based models, but these models can easily descend the flow, leading to the congestion state.

In scenario B, the Oscillation at the bottleneck occurred in all three models (**Fig. 15**), same as the Antoine's experiment [4], another result that we can conclude is that the Ellipse and Dynamic Ellipse models make the oscillations happen more frequently.

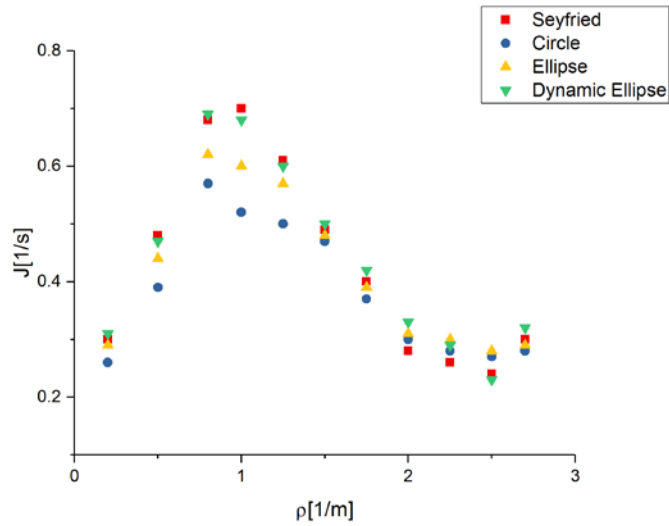


Fig. 16. Flow-density fundamental diagram in Scenario A. The dynamic ellipse model has the closest result to the empirical result.

3.2 The Influence of the Slow Reaction

We conduct the experiment before and after adding slow reaction state to the velocity-based model, then we compared the two results with Seyfried’s empirical result. The experiment set up in scenario 1, and the pedestrian number $N = 60$. When we set $p_i = 1$, the model is the origin velocity-based model, we select $p_i = 0.1, 0.3, 1$. The result (Fig. 17) revealed that when setting $p_i = 0.3$ the Slow Reaction model is much closer to the empirical result.

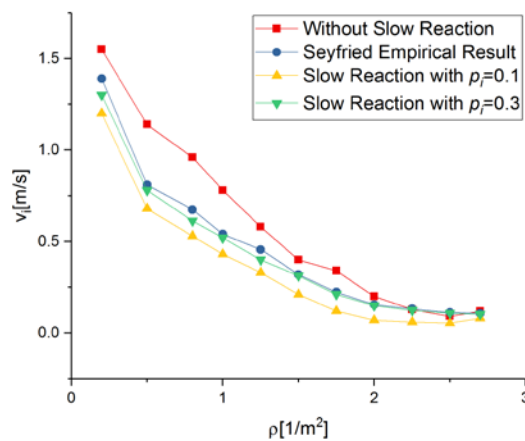


Fig. 17. Velocity-density fundamental diagram, different slow reaction parameter corresponding to different line.

In addition, we compared our model with the force-based model, the result is shown in [Fig. 18](#). We can conclude that when the density is low, the dynamic-ellipse model is closer to Seyfried's empirical result, as the density growing, the force-based model is getting closer to empirical result. So the force-based model has a good performance when pedestrian are tight together.

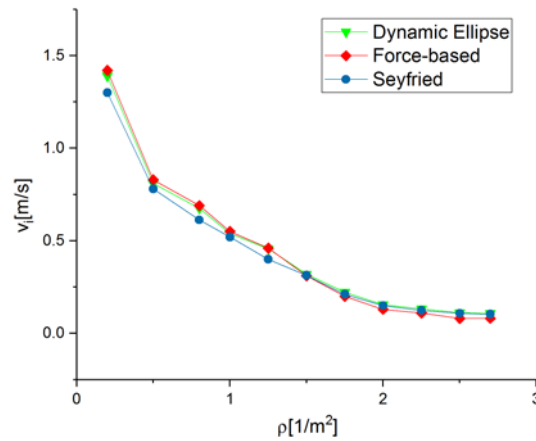


Fig. 18. Compared with the force-based models, the dynamic-ellipse model performed well in low density crowd.

3.3 The Different Initial Distributions

The three initial distributions of the pedestrian is applied to the velocity-based model with dynamic-ellipse shape. The experiment scene is similar to scenario 1, but it is larger, length $L = 25m$, width $W = 10m$. The pedestrian number is set to $N = 500,200$, $N(t)$ is the current moving pedestrian number in the scenario at a certain moment. We compared the evacuation efficiency and found out the exponential distribution has best efficiency shown in [Fig. 19](#). We found an interesting result that when the number of pedestrians is small enough relative to the scenario area, the pedestrian number would have a linear decrease.

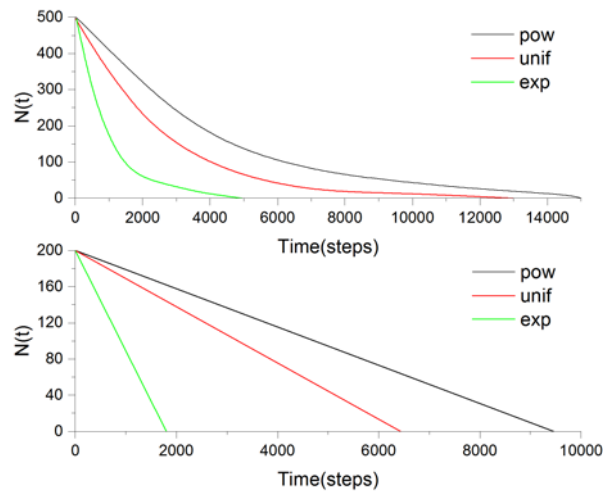


Fig. 19. The evacuation efficiency of three different distributions, the first figure is with 500 pedestrians and the second figure is with 200 pedestrians, the exponential distribution has the best evacuation efficiency.

4. Conclusion

In summary, the dynamic ellipse velocity-based model was proposed for pedestrian dynamics, the Dynamic ellipse velocity-based model has a better robustness than the force-based model in terms of pedestrian density.

We compared three velocity-based models with different shapes of the pedestrian. Our experiment is based on simulations, the main parameters are similar to Antoine's experiment, for ellipse and dynamic ellipse model, there are two pedestrian length parameters, the dynamic ellipse has a length parameter correlated with pedestrian speed. Then, we join the Slow Reaction model in the velocity-based model, bring in Slow Reaction coefficient p_i , the experiment result is much closer to the empirical data.

Also, we analyze the influence of the initial distribution to pedestrian dynamics, however, our experiment is not so complete, the result has some limitations, and may not be versatile to all scenarios. The pedestrian simulation system should be more persuasive by logical validation tools, such as [26] [27] [28] [29].

Ellipse with velocity-dependent radius emulates the space requirement of the projected shape of pedestrians better. In the future, the large and complex scenarios with great quantities of pedestrians would be a popular research direction, which is an important part of the Intelligent.

References

- [1] U. K. Mohcine Chraibi, Andreas Schadschneider, Armin Seyfried, "Force-based models of pedestrian dynamics," *Networks and Heterogeneous Media*, vol. 6, no. 3, pp. 17, September 2011. [Article \(CrossRef Link\)](#).
- [2] M. Chraibi, "Validated force-based modeling of pedestrian dynamics," *Dissertation / PhD ThesisBook, Schriften des Forschungszentrums Julich : IAS Series, Forschungszentrum Julich*, Zentralbibliothek, Julich, 2012. [Article \(CrossRef Link\)](#).
- [3] M. Chraibi, A. Tordeux, and A. Schadschneider, "A force-based model to reproduce stop-and-go waves in pedestrian dynamics," *Physics*, 2015. [Article \(CrossRef Link\)](#).
- [4] M. Chraibi, A. Seyfried, and A. Tordeux, "Collision-free speed model for pedestrian dynamics." [Article \(CrossRef Link\)](#).
- [5] F. Dietrich, and G. Köster, "Gradient navigation model for pedestrian dynamics," *Physical Review E*, vol. 89, no. 6, pp. 062801, 06/03/, 2014. [Article \(CrossRef Link\)](#).
- [6] J. Ondrejka, J. Pettr, Anne-H. n. Olivier, St, and p. Donikian, "A synthetic-vision based steering approach for crowd simulation," *ACM Trans. Graph.*, vol. 29, no. 4, pp. 1-9, 2010. [Article \(CrossRef Link\)](#).
- [7] P. Fiorini, "Motion planning in dynamic environments using velocity obstacles," *International Journal of Robotics Research*, vol. 17, pp. 760-772, 1998, 1998. [Article \(CrossRef Link\)](#).
- [8] A. Schadschneider, W. Klingsch, H. Klüpfel, T. Kretz, C. Rogsch, and A. Seyfried, "Evacuation Dynamics: Empirical Results, Modeling and Applications," *Extreme Environmental Events: Complexity in Forecasting and Early Warning*, R. A. Meyers, ed., pp. 517-550, New York, NY: Springer New York, 2011. [Article \(CrossRef Link\)](#).
- [9] J. Fang, Z. Qin, H. Hu, Z. Xu, and H. Li, "The fundamental diagram of pedestrian model with slow reaction," *Physica A: Statistical Mechanics and its Applications*, vol. 391, no. 23, pp. 6112-6120, 12/1/, 2012. [Article \(CrossRef Link\)](#).
- [10] A. Seyfried, M. Boltes, J. Kähler, W. Klingsch, A. Portz, T. Rupperecht, A. Schadschneider, B. Steffen, and A. Winkens, "Enhanced empirical data for the fundamental diagram and the flow through bottlenecks," *Physics*, 2008. [Article \(CrossRef Link\)](#).
- [11] A. Seyfried, B. Steffen, W. Klingsch, T. Lippert, and M. Boltes, "The Fundamental Diagram of Pedestrian Movement Revisited - Empirical Results and Modelling," 2007. [Article \(CrossRef Link\)](#).
- [12] J. Zhang, "Pedestrian fundamental diagrams: Comparative analysis of experiments in different geometries," *Dissertation / PhD Thesis, Schriften des Forschungszentrums Jülich : IAS Series*, Universität Wuppertal, Jülich, 2012. [Article \(CrossRef Link\)](#).
- [13] M. Bando, K. Hasebe, A. Nakayama, A. Shibata, and Y. Sugiyama, "Dynamical model of traffic congestion and numerical simulation," *Physical Review E*, vol. 51, no. 2, pp. 1035-1042, 02/01/, 1995. [Article \(CrossRef Link\)](#).

- [14] A. Nakayama, K. Hasebe, and Y. Sugiyama, "Instability of pedestrian flow and phase structure in a two-dimensional optimal velocity model," *Physical Review E*, vol. 71, no. 3, pp. 036121, 03/18/, 2005. [Article \(CrossRef Link\)](#).
- [15] D. Helbing, and P. Molnar, "Social Force Model for Pedestrian Dynamics," *Physics*, 1998. [Article \(CrossRef Link\)](#).
- [16] J. L. Pauls, "SUGGESTIONS ON EVACUATION MODELS AND RESEARCH QUESTIONS," 2004. [Article \(CrossRef Link\)](#).
- [17] D. R. Parisi, and C. O. Dorso, "Morphological and dynamical aspects of the room evacuation process," *Physica A: Statistical Mechanics and its Applications*, vol. 385, no. 1, pp. 343-355, 11/1/, 2007. [Article \(CrossRef Link\)](#).
- [18] A. Seyfried, B. Steffen, and T. Lippert, "Basics of modelling the pedestrian flow," *Physica A: Statistical Mechanics and its Applications*, vol. 368, no. 1, pp. 232-238, 8/1/, 2006. [Article \(CrossRef Link\)](#).
- [19] S. C. Benjamin, N. F. Johnson, and P. M. Hui, "Cellular automata models of traffic flow along a highway containing a junction," *Physics*, 1996. [Article \(CrossRef Link\)](#).
- [20] N. MOUSSA, "EVACUATION PROCESS IN TWO-DIMENSIONAL TRAFFIC FLOW MODELS," *International Journal of Modern Physics B*, vol. 23, no. 02, pp. 169-176, 2009. [Article \(CrossRef Link\)](#).
- [21] S. H. A. S. H. Bouk, D. Kim and H. Song, "Named-Data-Networking-Based ITS for Smart Cities," *IEEE Communications Magazine*, vol. 55, January 2017, 2017. [Article \(CrossRef Link\)](#).
- [22] W. Li, and H. Song, "ART: An Attack-Resistant Trust Management Scheme for Securing Vehicular Ad Hoc Networks," *IEEE Transactions on Intelligent Transportation Systems*, vol. 17, no. 4, pp. 960-969, 2016. [Article \(CrossRef Link\)](#).
- [23] T. Kretz, A. Grunebohm, and M. Schreckenberg, "Experimental study of pedestrian flow through a bottleneck," *Statistics*, 2006. [Article \(CrossRef Link\)](#).
- [24] A. Seyfried, T. Rupperecht, O. Passon, B. Steffen, W. Klingsch, and M. Boltes, "New insights into pedestrian flow through bottlenecks," *Physics*, 2007. [Article \(CrossRef Link\)](#).
- [25] M. Chraibi, A. Seyfried, and A. Schadschneider, "Generalized centrifugal-force model for pedestrian dynamics," *Physical Review E*, vol. 82, no. 4, pp. 046111, 10/20/, 2010. [Article \(CrossRef Link\)](#).
- [26] Y. Jiang, Z. Li, H. Zhang, Y. Deng, X. Song, M. Gu, and J. Sun, "Design and optimization of multiclocked embedded systems using formal techniques," *IEEE Transactions on Industrial Electronics*, 62(2):1270-1278, 2015. [Article \(CrossRef Link\)](#).
- [27] Y. Jiang, H. Zhang, X. Song, X. Jiao, W. N. N. Hung, M. Gu, and J. Sun, "Bayesian-Network-Based Reliability Analysis of PLC Systems," *IEEE Transactions on Industrial Electronics*, vol. 60, no. 11, pp. 5325-5336, 2013. [Article \(CrossRef Link\)](#).

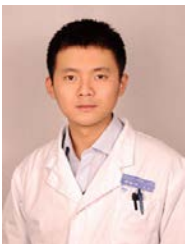
- [28] Y. Jiang, H. Zhang, H. Zhang, H. Liu, X. Song, M. Gu, and J. Sun, "Design of Mixed Synchronous/Asynchronous Systems with Multiple Clocks," *IEEE Transactions on Parallel and Distributed Systems*, vol. 26, no. 8, pp. 2220-2232, 2015. [Article \(CrossRef Link\)](#).
- [29] Y. Jiang, H. Song, R. Wang, M. Gu, J. Sun, and L. Sha, "Data-Centered Runtime Verification of Wireless Medical Cyber-Physical System," *IEEE Transactions on Industrial Informatics*, vol. PP, no. 99, pp. 1-1, 2016. [Article \(CrossRef Link\)](#).



Xiao Yang received his M.S. degree in the Department of NUDT of China, in December 2011. He is currently working towards his Ph.D. degree in Software Engineering at Tsinghua University, China. Currently, His research interests include Pedestrian evacuation dynamics, Intelligent Transportation Systems, and Pattern Recognition.



Zheng Qin is a doctoral supervisor, professor, the Director of Software Engineering and Management Research Institute and Information Institute, Tsinghua University. He is the evaluation expert of The Recruitment Program of Global Experts, holder of the National Science and Technology Award of the Ministry of Education of Technology Award. Currently his research interests include pedestrian dynamics, Mobile computing, E-commerce Computer vision and Network security.



Binhua Wan received the M.S. degree in Peking university and bachelor's degree in the capital university of medical sciences, his interesting subject include clinical medicine.



Renwei Zhang received the M.S. degree in Software Engineering from Peking University, Beijing, China, in July 2012. He is now a Ph.D. candidate in school of Software Engineering, Tsinghua University, Beijing. His research interests are software testing, model driven engineering, model versioning, and so on.



Huihui Wang is Assistant Professor and Chair of Department of Engineering, Jacksonville University, Jacksonville, Healthcare and medical engineering based on smart materials, Haptics based on smart materials /structures, Cyber-Physical Systems, and MEMS.